An OFDM Symbol Design for Reduced Complexity MMSE Channel Estimation

Carlos Ribeiro
Instituto Politécnico de Leiria/Escola Superior de Tecnologia e Gestão, Leiria, Portugal
Email: cribeiro@estg.ipleiria.pt

Atílio Gameiro
Universidade de Aveiro/Instituto de Telecomunicações, Aveiro, Portugal
Email: amg@ua.pt

Abstract—**In this paper we revisit the minimum mean square error (MMSE) pilot-aided channel estimation for broadband orthogonal frequency division multiplexing (OFDM) systems. The careful design of OFDM symbol leads to the proposal of a simplified time-domain (TD) MMSE estimator. By exploring the Fourier properties of the symbol, the investigated method eliminates the need to use direct or inverse discrete Fourier transforms (DFT/IDFT) before the channel estimation, by using the TD received symbol samples as the input to the MMSE filter. Moreover, performing the estimation in TD (where the channel impulse response (CIR) energy is mainly limit to a small set of samples), makes way to a simple, nonetheless efficient estimation of the filter parameters. The performance of the channel estimation scheme, using the estimated parameters, presents a tolerable degradation when compared with the ideal situation (*a-priori* knowledge of the channel correlation and noise variance), while exhibiting a reduced computational load. The feasibility of the investigated method is substantiated by system simulation using indoor and outdoor wireless channel models.**

Index Terms—**OFDM, pilot-aided channel estimation, time-domain processing.**

I. INTRODUCTION

Future mobile broadband applications will require reliable high data-rate wireless communication systems. In recent years, OFDM-based transmission systems [1]-[3] emerged as the scheme with the potential to fulfill these conditions, with bandwidth efficiency and robustness to frequency selective channels, common in mobile personal communication systems.

Extraction of accurate channel state information is crucial to achieve high spectral efficiency, with emphasis on demodulation/decoding and resource allocation operations. MMSE-based pilot-aided channel estimators, either in TD [4] or frequency-domain (FD) [5], exhibit the best performance in the presence of Additive White Gaussian Noise (AWGN), if the receiver has *a-priori* knowledge of the channel correlation and noise variance. Since this information is not available, finding the most robust estimator to channel correlation mismatches [6] and tracking the channel changes grew to be main design topics.

The parametric channel modeling has been developed to represent sparse multipath fading channels [7]. The tracking of a reduced dimension signal subspace of the channel correlation matrix (built from the parametric channel model) has been the focus of several works [7]-[9]. These pilot-aided parametric channel estimation methods achieve low mean square error (MSE) values for the span of signal-to-noise ratios (SNR), but have the inevitable drawback of a relevant computational load.

Published work on TD channel estimation [10]-[11] put in evidence that the estimation process can be performed directly in TD, processing the received serial signal. However, due to the common FD pilot arrangement, most of the publications on the topic of pilot-aided channel estimation use the FD *least squares* (LS) estimates (back-rotated received signal) as the starting point for the estimation process. It was demonstrated that this operation can be performed in TD by a simple linear operation on the received signal [12]. This fact gives rise to the use of an MMSE estimator filter whose input is directly linked to the received symbol samples with no DFT/IDFT operations performed before the estimation filter [4]. Furthermore, the effective size of the matrices involved in the filtering can be significantly reduced with minimum error.

This paper contains a proposal for a pilot-aided TD MMSE channel estimator for OFDM systems where pilots are multiplexed along with data symbols in different sub-carriers within the OFDM symbol. The estimator structure is undemanding and the complexity reduced. Utilizing an initial TD channel estimate, the method uses a simple scheme to estimate the MMSE filter parameters: the slowly-varying delays of the multipath channel and the noise variance.

The paper is organized as follows. Next section gives a brief introduction to the wireless multipath channel and the OFDM baseband model. In section III, the investigated channel estimation algorithm is developed. The feasibility of the new method is substantiated by

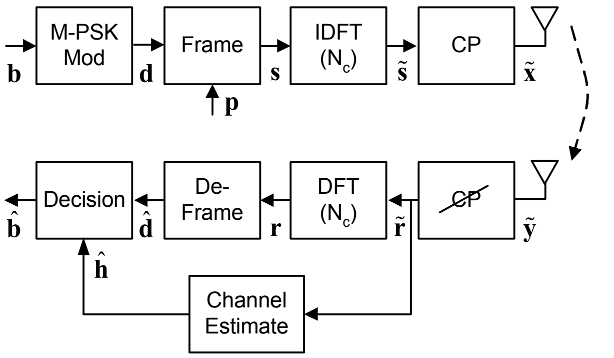

Figure 1. OFDM baseband system model.

simulation results presented in section IV. Finally, conclusions are drawn in section V.

II. OFDM in Mobile Wireless Channels

Before introducing the investigated method, we will briefly overview the mobile wireless multipath channel and the considered OFDM baseband model.

Throughout the text, the notation $(\tilde{\ })$ is used for TD vectors and elements and its absence denotes FD vectors and elements. The index *n* denotes TD elements and *k* FD elements. Unless stated otherwise, the vectors involved in the transmission/reception process are column vectors with N_C complex elements. The superscripts $(.)^T$ and $(.)^H$ denote transpose and Hermitian transpose, respectively.

A. The Wireless Multipath Channel

Let's consider that the system transmits over a multipath Rayleigh fading wireless channel, modeled by the discrete-time CIR

$$\tilde{h}[n] = \sum_{l=0}^{L-1} \alpha_l \delta[n-\tau_l], \quad (1)$$

where L is the number of channel paths, α_l and τ_l are the complex value and delay of path *l*, respectively. The paths are assumed to be statistically independent, with normalized average power, $\sum_{l=0}^{L-1} \sigma_h^2[l] = 1$, where $\sigma_h^2[l]$ is the average power of path *l*. The channel is time-variant due to the motion of the mobile terminal (MT), but we will assume that the CIR is constant during one OFDM symbol. The time dependence of the CIR is not present in the notation for simplicity. Assuming that the insertion of a long enough cyclic prefix (CP) in the transmitter assures that the orthogonality of the sub-carriers is maintained after transmission, the channel frequency response (CFR) can be expressed as

$$h[k] = \sum_{l=0}^{L-1} \alpha_l \exp\left[-j\frac{2\pi}{N_C} k\tau_l\right], \quad (2)$$

where N_C is the total number of sub-carriers of the OFDM system.

B. OFDM Baseband Model

Let's consider the OFDM baseband system with N_C sub-carriers depicted in Fig. 1. At time *n*, the binary data vector **b** is *M*-ary PSK or QAM modulated into vector **d**.

To assist in the channel estimation process, pilot symbols are multiplexed together with data symbols in different sub-carriers. The pilot symbols are collected in vector **p**.

Vectors **p** and **d** contain non-zero values at disjoint positions (sub-carriers). The resulting FD vector is $\mathbf{s} = \mathbf{d} + \mathbf{p}$.

The IDFT block transforms the input vector into the TD vector $\tilde{\mathbf{s}}$, using an efficient N_C-points inverse fast Fourier transform (FFT) algorithm.

An *L* samples long guard interval, in the form of CP, is prefixed to vector $\tilde{\mathbf{s}}$, resulting in the TD transmitted vector

$$\tilde{\mathbf{x}} = \mathbf{A}_{CP}\mathbf{F}^H\mathbf{s} = \mathbf{A}_{CP}\left(\tilde{\mathbf{d}} + \tilde{\mathbf{p}}\right), \quad (3)$$

where $\mathbf{F} \triangleq N_C^{-1/2}\left(e^{-j2\pi kn/N_C}\right)_{k,n=0,0}^{N_C-1,N_C-1}$ is the $N_C \times N_C$ DFT matrix and $\mathbf{A}_{CP} = \left[\mathbf{I}_{N_C\times L} \ \ \mathbf{I}_{N_C}\right]^T$ is the matrix that adds the CP, with $\mathbf{I}_{N_C}$ denoting the $N_C \times N_C$ identity matrix and $\mathbf{I}_{N_C\times L}$ denoting the last *L* columns of $\mathbf{I}_{N_C}$. The TD vectors $\tilde{\mathbf{d}}$ and $\tilde{\mathbf{p}}$ collect, respectively, the components of the data symbols and pilot symbols present in $\tilde{\mathbf{s}}$.

The transmission over an uncorrelated wireless channel results in the received signal

$$\tilde{\mathbf{y}} = \tilde{\mathbf{H}}'\tilde{\mathbf{x}} + \tilde{\mathbf{w}}', \quad (4)$$

where the vector $\tilde{\mathbf{w}}'$ is made-up of independent and identically distributed (*iid*) zero mean AWGN samples with variance σ_w^2. The matrix $\tilde{\mathbf{H}}'$ is the $(N_C+L)\times(N_C+L)$ lower triangular Toeplitz channel convolution matrix with first column $\left[\tilde{\mathbf{h}}^T \ \ \mathbf{0}_{1\times N_C}\right]^T$, where $\tilde{\mathbf{h}}$ is the column *L*-vector with the discrete-time CIR (its elements are defined by (1)) and $\mathbf{0}_{1\times N_C}$ is a null N_C-vector.

The receiver starts by removing the CP from each symbol. The resulting vector for symbols with pilots and data is

$$\begin{aligned}\tilde{\mathbf{r}} &= \mathbf{R}_{CP}\tilde{\mathbf{y}} = \mathbf{R}_{CP}\tilde{\mathbf{H}}'\mathbf{A}_{CP}\left(\tilde{\mathbf{d}} + \tilde{\mathbf{p}}\right) + \mathbf{R}_{CP}\tilde{\mathbf{w}}' \\ &= \tilde{\mathbf{H}}\left(\tilde{\mathbf{d}} + \tilde{\mathbf{p}}\right) + \tilde{\mathbf{w}}\end{aligned}, \quad (5)$$

where $\mathbf{R}_{CP} = \left[\mathbf{0}_{N_C\times L} \ \ \mathbf{I}_{N_C}\right]$ is the matrix that removes the CP, $\tilde{\mathbf{w}} = \mathbf{R}_{CP}\tilde{\mathbf{w}}'$ is the resulting TD noise vector and

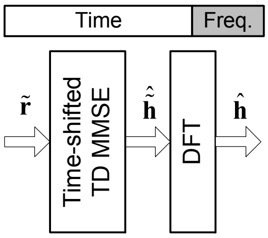

Figure 2. TD pilot-aided MMSE channel estimation.

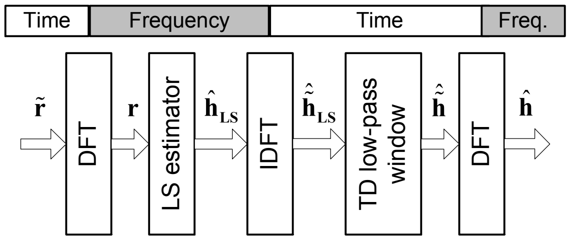

Figure 3. Pilot-aided DFT-based channel estimator.

$\tilde{\mathbf{H}} = \mathbf{R}_{CP}\tilde{\mathbf{H}}'\mathbf{A}_{CP}$ is the $N_C \times N_C$ circulant matrix with circulant vector $\begin{bmatrix}\tilde{\mathbf{h}}^T & \mathbf{0}_{1\times(N_C-L)}\end{bmatrix}^T$. The vector $\tilde{\mathbf{r}}$ is the input to both DFT and channel estimation blocks.

The channel estimation block uses the pilot component present in $\tilde{\mathbf{r}}$ for the estimation process. The output vector $\hat{\mathbf{h}}$ consists of the FD channel estimates for all sub-carriers.

The DFT block transforms vector $\tilde{\mathbf{r}}$ to FD with an efficient FFT operation. The resulting FD column N_C-vector can be expressed as

$$\mathbf{r} = \mathbf{F}\tilde{\mathbf{r}} = \mathbf{H}(\mathbf{d}+\mathbf{p}) + \mathbf{w}, \tag{6}$$

where, due to the properties of the DFT, $\mathbf{H}$ is a $N_C \times N_C$ diagonal matrix whose diagonal elements are defined by (2) and $\mathbf{w}$ is the FD noise vector.

The de-framing block separates the signals in the sub-carriers conveying pilots and data symbols. The values in the data sub-carriers are collected in vector $\hat{\mathbf{d}}$ and fed to the decision block. Together with the channel estimate, the decision block is now able to decide what where the transmitted symbols, according to some decision rule, and generate the estimate of the transmitted data $\hat{\mathbf{b}}$.

III. OFDM Symbol Desing for Reduced Complexity MMSE Channel Estimation

The proposed method estimates the channel from the TD received symbols carrying pilots and data, taking advantage of the properties of the designed OFDM symbol (Fig. 2). Extending the results in [12] to the use of a TD MMSE criterion, all the processing required to estimate the CIR is performed immediately in TD. It eliminates the need to move from TD to FD and back to TD to finally obtain the CIR estimate, common to the methods in [4], [13]-[15] (Fig. 3). The simple TD operation succeeds in simultaneously remove the data-dependent component in $\tilde{\mathbf{r}}$, generate the TD LS channel estimate and improve this initial estimate using the TD MMSE criterion, that optimally weighs the average power of the CIR taps to the noise variance.

A. Design of the OFDM Symbol

Consider the set of sub-carriers $\wp$ dedicated to convey pilot symbols,

$$\wp = \{0, N_f, 2N_f, \cdots, N_C - N_f\}, \tag{7}$$

where the pilot distance N_f can range from 1 (particular case where all sub-carriers in the OFDM symbol are dedicated to transmit pilots – training symbol) to N_C, fulfilling the condition

$$\frac{N_C}{N_f} = N_t \in \mathbb{N}. \tag{8}$$

The transmitted pilots all have equal value (without loss of generality, in following, the pilots will have the value "1"), resulting in the *k*-th element of the pilot vector $\mathbf{p}$,

$$p[k] = \sum_{m=0}^{N_t-1} \delta\left[k - mN_f\right]. \tag{9}$$

Conversely, the *n*-th element of the corresponding TD vector $\tilde{\mathbf{p}}$ is

$$\begin{aligned}\tilde{p}[n] &= \begin{cases} \frac{1}{N_f}, & \text{if } n = mN_t,\ \ m = 0,1,..,N_f-1 \\ 0, & \textit{remaining} \end{cases} \\ &= \frac{1}{N_f}\sum_{m=0}^{N_f-1}\delta\left[n - mN_t\right]\end{aligned} \tag{10}$$

The *n*-th element of $\tilde{\mathbf{d}}$ can be expressed by

$$\tilde{d}[n] = N_C^{-1/2}\sum_{\substack{k=0\\k\notin\wp}}^{N_C-1} d[k]e^{j2\pi\frac{kn}{N_C}}, \tag{11}$$

where $d[k]$ is the *k*-th element of $\mathbf{d}$ (complex data symbol conveyed by the *k*-th sub-carrier).

Using equations (10) and (11), the *n*-th element of $\tilde{\mathbf{r}}$ is

$$\tilde{r}[n] = \sum_{l=0}^{L-1}\tilde{h}[l]\tilde{d}[n-l] + \frac{1}{N_f}\sum_{m=0}^{N_f-1}\tilde{h}[n-mN_t] + \tilde{w}[n]. \tag{12}$$

Equation (12) puts in evidence that the received signal is the sum of three distinct components: the data vector $\tilde{\mathbf{d}}$ and pilot vector $\tilde{\mathbf{p}}$ transmitted over the wireless channel, and the AWGN. Looking carefully at the component dependent on the pilot vector, it becomes clear that it is made-up of N_f scaled replicas of the CIR. Moreover, the CIR replicas are separated by N_t samples.

Given the normalized channel bandwidth $\frac{\tau_{\max}}{N_C \Delta t}$, where $\tau_{\max}$ is the maximum channel delay spread and Δt is the sampling interval, the minimum pilot distance N_f that can be used with no overlap in adjacent channel replicas, thus enabling the best performance of the channel estimator, is

$$N_f \leq \frac{N_C \Delta t}{\tau_{\max}}. \tag{13}$$

Otherwise, the overlapping of consecutive replicas will cause distortion in the estimation process and impose an irreducible MSE floor on the estimate.

B. Time Analysis of DFT-based Channel Estimation

Let's briefly perform a TD analysis of the operations of the DFT-based channel estimator [13] depicted in Fig. 3, when using the OFDM symbol design of the previous section. The estimator initiates by transforming the TD vector $\tilde{\mathbf{r}}$ into the FD vector $\mathbf{r}$ using a DFT operation. It proceeds with the FD LS estimation of sub-carriers conveying pilots. The k-th element of the LS estimate vector $\hat{\mathbf{h}}_{\mathbf{LS}}$ is

$$\hat{h}_{LS}[k] = r[k] \sum_{m=0}^{N_t-1} \delta\left[k - mN_f\right]. \tag{14}$$

The LS estimate vector is transformed to TD with the use of an IDFT operation, $\hat{\tilde{\mathbf{h}}}_{\mathbf{LS}} = \mathbf{F}^H \hat{\mathbf{h}}_{\mathbf{LS}}$. The n-th element of the resulting vector is

$$\begin{aligned}\hat{\tilde{h}}_{LS}[n] &= N_C^{-1/2} \sum_{k=0}^{N_C-1} r[k] \sum_{m=0}^{N_t-1} \delta\left[k - mN_f\right] \exp\left[j\frac{2\pi}{N_C}kn\right] \\ &= \frac{1}{N_f}\sum_{m=0}^{N_f-1} \tilde{h}\left[n - mN_t\right] + \tilde{w}_{LS}[n]\end{aligned}, \tag{15}$$

where the noise component $\tilde{w}_{LS}[n]$ is defined by

$$\tilde{w}_{LS}[n] = N_C^{-1/2} \sum_{k\in\wp} w[k] \exp\left[j\frac{2\pi}{N_C}kn\right]. \tag{16}$$

The TD rectangular low-pass window $\tilde{\mathbf{t}}$, defined by

$$\tilde{t}[n] = N_f\left(u[n] - u[n - N_t + 1]\right), \tag{17}$$

is used to select the first CIR replica present in $\hat{\tilde{\mathbf{h}}}_{\mathbf{LS}}$ and thus attain the CIR estimate vector $\hat{\tilde{\mathbf{h}}}$,

$$\begin{aligned}\hat{\tilde{h}}[n] &= \tilde{t}[n]\hat{\tilde{h}}_{LS}[n] \\ &= \begin{cases}\tilde{h}[n] + N_f \tilde{w}_{LS}[n], & n = 0,\cdots,N_t - 1 \\ 0, & remaining\end{cases}\end{aligned}. \tag{18}$$

The CFR estimate vector $\hat{\mathbf{h}}$ is the result of transforming the CIR estimate back to FD, $\hat{\mathbf{h}} = \mathbf{F}\hat{\tilde{\mathbf{h}}}$.

C. Attaining the CIR estimate from the TD samples

Considering that the condition in (13) is fulfilled, an adequate processing that succeeds in removing the data dependent component from (12) would open way to easily obtain estimates of the CIR immediately from the received vector $\tilde{\mathbf{r}}$. The operation that achieves this goal is [12]

$$\hat{\tilde{\mathbf{h}}} = \mathbf{T}\tilde{\mathbf{r}}, \tag{19}$$

where the $(N_t \times N_C)$ matrix $\mathbf{T} = \left[\mathbf{I}_{N_t} \cdots \mathbf{I}_{N_t}\right]$. The n-th element of $\hat{\tilde{\mathbf{h}}}$ is

$$\begin{aligned}\hat{\tilde{h}}[n] &= \begin{cases}\sum_{m=0}^{N_f-1} \tilde{r}[n + mN_t], & n = 0,\cdots,N_t - 1 \\ 0, & remaining\end{cases} \\ &= \left(u[n] - u[n - N_t + 1]\right)\sum_{m=0}^{N_f-1} \tilde{r}[n + mN_t] \\ &= \left(u[n] - u[n - N_t + 1]\right)\times \\ &\times\left(\begin{aligned}&\frac{1}{N_f}\sum_{m=0}^{N_f-1}\sum_{l=0}^{N_f-1}\tilde{h}\left[n + (m-l)N_t\right] + \sum_{m=0}^{N_f-1}\tilde{w}[n + mN_t] \\ &+ \frac{1}{N_f}\sum_{m=0}^{N_f-1}\sum_{l=0}^{L-1}\tilde{h}[l]\tilde{d}[n + mN_t - l]\end{aligned}\right) \\ &= \begin{cases}\tilde{h}[n] + N_f\tilde{w}_{LS}[n], & n = 0,\cdots,N_t - 1 \\ 0, & remaining\end{cases}\end{aligned} \tag{20}$$

The last step in (20) was possible considering that the data component was eliminated due to the fact that

$$\begin{aligned}&\frac{1}{N_f}\sum_{m=0}^{N_f-1}\sum_{l=0}^{L-1}\tilde{h}[l]\tilde{d}[n + mN_t - l] = \\ &= \frac{N_C^{-1/2}}{N_f}\sum_{l=0}^{L-1}\tilde{h}[l]\sum_{\substack{k=0 \\ k\notin\wp}}^{N_C-1} d[k]\exp\left[j\frac{2\pi}{N_C}k(n-l)\right]\times \\ &\times\sum_{m=0}^{N_f-1}\exp\left[j\frac{2\pi}{N_C}kmN_t\right] = 0\end{aligned} \tag{21}$$

The result in (21) is best understood considering that only the sub-carriers $k \in \wp$ add constructively in the operation performed in (20). Correspondingly, the resulting noise component in (20) is justified considering that

$$\begin{aligned}&\sum_{m=0}^{N_f-1}\tilde{w}[n + mN_t] \\ &= N_C^{-1/2}\sum_{k=0}^{N_C-1} w[k]\exp\left[j\frac{2\pi}{N_C}kn\right]\sum_{m=0}^{N_f-1}\exp\left[j\frac{2\pi}{N_C}kmN_t\right] \\ &= N_f N_C^{-1/2}\sum_{k\in\wp} w[k]\exp\left[j\frac{2\pi}{N_C}kn\right] = N_f\tilde{w}_{LS}[n]\end{aligned}. \tag{22}$$

The result in (20) demonstrates that the simple operation in (19) yields the same CIR estimate attained by (18).

D. MMSE Smoothing Filter

The initial CIR estimate of (19) can be improved with the use of a smoothing filter. With the knowledge that the CIR energy is limited to the set of taps $\{L\}$, with L elements, an MMSE filter will optimally weigh the CIR energy to the noise variance inside this set and remove the outside noise, so to achieve the lowest possible estimate MSE.

The MMSE filter is implemented by the $(N_t \times N_t)$ matrix [16]

$$\mathbf{W} = \mathbf{R}_{h\hat{h}} \mathbf{R}_{\hat{h}\hat{h}}^{-1}, \tag{23}$$

where the $(N_t \times N_t)$ filter input correlation matrix is

$$\mathbf{R}_{\hat{h}\hat{h}} = E\left\{\hat{\hat{\mathbf{h}}}\hat{\hat{\mathbf{h}}}^H\right\} = \mathbf{R}_{hh} + \frac{\sigma_w^2}{N_t}\mathbf{I}_{N_t}, \tag{24}$$

and the $(N_t \times N_t)$ filter input–output cross-correlation matrix is

$$\mathbf{R}_{h\hat{h}} = E\left\{\tilde{\mathbf{h}}\hat{\hat{\mathbf{h}}}^H\right\} = \mathbf{R}_{hh}, \tag{25}$$

with the $(N_t \times N_t)$ channel correlation diagonal matrix

$$\mathbf{R}_{hh} = E\{\tilde{\mathbf{h}}\tilde{\mathbf{h}}^H\} = diag\left(\left[\sigma_h^2[0], \cdots, \sigma_h^2[L-1], 0, \cdots, 0\right]\right). \tag{26}$$

Replacing equations (24) to (26) in (23), the MMSE filter becomes,

$$\mathbf{W} = diag\left(\left[\frac{\sigma_h^2[0]}{\sigma_h^2[0] + \frac{\sigma_w^2}{N_t}}, \cdots, \frac{\sigma_h^2[L-1]}{\sigma_h^2[L-1] + \frac{\sigma_w^2}{N_t}}, 0, \cdots, 0\right]\right). \tag{27}$$

The final CIR estimate can be expressed by

$$\hat{\hat{\mathbf{h}}}_{MMSE} = \mathbf{W}\hat{\hat{\mathbf{h}}}. \tag{28}$$

Taking into consideration that the filter is implemented with a diagonal matrix with L non-zero elements, the MMSE filtering in (28) can be performed simultaneously with the operation in (19). In fact, the merge of both operations reduces the computational load of (19), by limiting the summation interval in (20) to the set $\{L\}$. The elements of the final CIR estimate can be found by

$$\hat{\hat{h}}_{MMSE}[n] = \begin{cases} \dfrac{\sigma_h^2[n]}{\sigma_h^2[n] + \frac{\sigma_w^2}{N_t}} \displaystyle\sum_{m=0}^{N_f-1} \tilde{r}[n + mN_t], & n \in \{L\} \\ 0, & remaining \end{cases}$$
$$= \begin{cases} \dfrac{\sigma_h^2[n]\left(\tilde{h}[n] + N_f \tilde{w}_{LS}[n]\right)}{\sigma_h^2[n] + \frac{\sigma_w^2}{N_t}}, & n \in \{L\} \\ 0, & remaining \end{cases}. \tag{29}$$

E. MMSE Filter Project

Examining (27) it is clear that the computation of the filter coefficients requires only L complex divisions, unlike its FD counterpart [5] that needs a computationally demanding full matrix inversion.

The MMSE filter is a function of two design parameters: the channel correlation matrix $\mathbf{R}_{hh}$ and the noise variance σ_w^2, none of which available to the receiver in a real scenario. Moreover, if the transmission is performed over a time-varying channel, these parameters must be tracked to maintain the filter's performance.

Making use of $\hat{\hat{\mathbf{h}}}$, where the CIR energy is limited to the set of taps $\{L\}$, the estimate of the filter parameter is significantly simplified when compared to other FD estimation methods [17].

The channel correlation matrix is dependent on the complex values and delays of the channel paths. The variation of the complex path values is linked to the Doppler shift, leading to considerable variations between consecutive symbols for high values of MT velocity.

On the other hand, the delays may be considered constant for the duration of t symbols provided that its variation $\Delta\tau$ is much smaller than the system's temporal resolution, $\Delta\tau \ll \Delta t$. For a radial movement between transmitter and receiver with velocity v, the variation of delay in t symbols is $\Delta\tau = \frac{vtT_s}{c}$, leading to

$$t \ll \frac{c\Delta t}{vT_s}, \tag{30}$$

where the speed of light $c = 3\times10^8 m/s$ and T_s is the OFDM symbol duration.

For $v = 100km/h$ and with the system parameters defined in the simulation results section, the delays can be considered constant for $t \approx 1000$ symbols.

Considering that the delays remain constant for q pilot-carrying symbols, we propose a simple method to estimate the slowly-varying delays $\hat{\tau}_l$ (and associated average power values $\hat{\sigma}_h^2[l]$) and noise variance $\hat{\sigma}_w^2$.

The estimation of the noise variance $\hat{\sigma}_w^2$ uses the samples $\left\{\hat{\hat{h}}[n],\ n \notin \{L\}\right\}$,

$$\hat{\sigma}_w^2 = \frac{N_t}{(N_t - L)q} \sum_{t=1}^{q} \sum_{n \notin \{L\}} \left|\hat{\hat{h}}_t[n]\right|^2. \tag{31}$$

The elements of the main diagonal of the channel correlation matrix $\mathbf{R}_{hh}$ are estimated by

$$\hat{\sigma}_h^2[n] = \frac{1}{q} \sum_{t=1}^{q} \sum_{n \in \{L\}} \left|\hat{\hat{h}}_t[n]\right|^2 - \frac{\hat{\sigma}_w^2}{N_t}. \tag{32}$$

On the simulation results presented in the next section, we have updated the filter parameters on every OFDM

TABLE I.
DFT CHANNEL ESTIMATION COMPLEXITY (OPS. PER SUB-CARRIER)

	LS Estimate	DFT / IDFT	TD weighting window	Required ops. per tap
Multiplic.	1	$\frac{\log_2(N_C)}{2}$	1	$2+\log_2(N_C)$
Addition	–	$\log_2(N_C)$	–	$2\log_2(N_C)$

frame. This option proved to be a good trade-off between computational load and estimation performance.

F. Complexity Analysis of TD-based Channel Estimators

The investigated method requires $\frac{L}{N_C}$ multiplications and $\frac{LN_f}{N_C}$ additions per tap to implement the time-shifted TD MMSE block, resulting in a total complexity per CFR sub-carrier of $\frac{L}{N_C}+\frac{\log_2(N_C)}{2}$ multiplications and $\frac{LN_f}{N_C}+\log_2(N_C)$ additions, if the complexity of the tracking procedure is discarded.

The complexity of the method in [13] is summarized in Table I. To calculate each CFR sub-carrier estimate it requires a total of $2+\log_2(N_C)$ multiplications and $2\log_2(N_C)$ additions. To further implement the TD MMSE method in [4] with a $N_t \times N_t$ MMSE matrix, it requires $\frac{N_t^2}{N_C}$ additional multiplications and equal number of additions, resulting in a total complexity of $1+\log_2(N_C)+\frac{N_t^2}{N_C}$ multiplications and $2\log_2(N_C)+\frac{N_t^2}{N_C}$ additions.

Table II compares the complexity between the investigated method and the methods in [4] and [13] for the indoor simulation scenario ($L=9$ taps channel) described in section IV. It puts in evidence the considerable computational load reduction achieved by the proposed method, with no performance trade-off.

G. Analysis of TD-based Channel Estimatiors' MSE

Assuming that the noise in the TD samples is *iid*, the noise variance in (19) is σ_w^2, resulting in the initial channel estimation MSE

$$MSE_{INI}=\sigma_w^2 . \tag{33}$$

By eliminating the noise in the samples where there is no CIR energy, the noise variance in the channel estimation method in [12] is reduced and the resulting channel estimation MSE is

TABLE II.
COMPLEXITY COMPARISON (OPS. PER SUB-CARRIER)

	TD MMSE	LS-DFT [13]	DFT+MMSE [4]
Multiplic.	≈5	12	75
Additions	≈10	20	85

$$MSE_{STC}=\sigma_w^2\frac{L}{N_t}=MSE_{INI}\frac{L}{N_t} . \tag{34}$$

This MSE tends to the initial MSE when L goes to N_t (limiting condition in (13)).

An error floor will limit the performance for high values of SNR if the set $\{L\}$ is not properly estimated and some CIR energy is removed.

In the investigated channel estimation method, the resulting MSE is [15]

$$MSE_{MMSE}=\sigma_w^2\frac{L}{N_t}\sum_{l\in\{L\}}\frac{\sigma_h^2[l]}{\sigma_h^2[l]+\frac{\sigma_w^2}{N_t}} . \tag{35}$$

Observing (35), we can conclude that when $SNR\to\infty$, $MSE_{MMSE}\to MSE_{STC}$. Results presented in the next section confirm this analysis.

IV. SIMULATION RESULTS

A simulation scenario was implemented where $N_C=1024$ sub-carriers were QPSK modulated. The system used a carrier frequency $f_C=5GHz$ and the sampling interval was set to $\Delta t=50ns$. The transmitted OFDM symbols carried pilots and data using the proposed pilot structure, with a pilot separation $N_f=4$. The OFDM frame consists of 24 symbols.

Two channel models with exponential decaying power delay profile (PDP) were used to simulate indoor ($50ns$ *rms* delay spread) and outdoor environments ($250ns$ *rms* delay spread).

To validate the proposed method, BER and channel estimation simulations were performed, using Eb/N0 values in the range of *0dB* to *20dB*. Its performance is plotted against the one of the methods in [12] and [13]. The proposed method is simulated using the ideal MMSE filter and using the estimated parameters. The method in [12] is simulated using the perfect set of delays $\{L\}$, that represents the upper bound on the method's performance.

The normalized channel estimation MSE results are depicted in Fig. 4 and Fig. 6, respectively for indoor and outdoor channels. The proposed method and the methods in [12] and [13] are noted as "TD MMSE", "TD STC" and "TD LS-DFT", respectively. The proposed method using the filter with estimated parameters in noted "TD MMSE (Param.Est.)".

The BER results are depicted in Fig. 5 and Fig. 7, respectively for indoor and outdoor channels. The plot

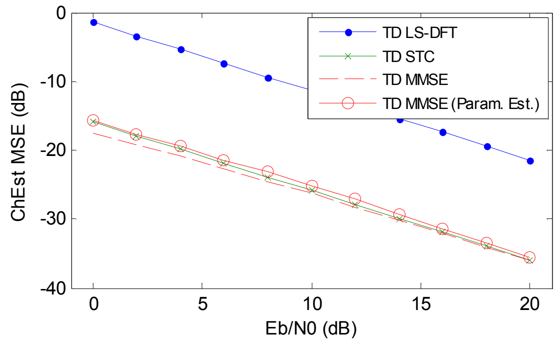

Figure 4. Channel estimation MSE (indoor scenario).

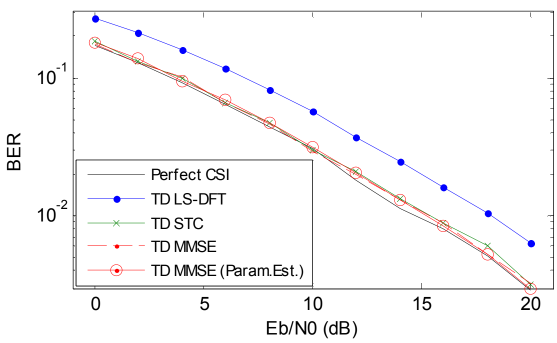

Figure 5. System BER performance (indoor scenario).

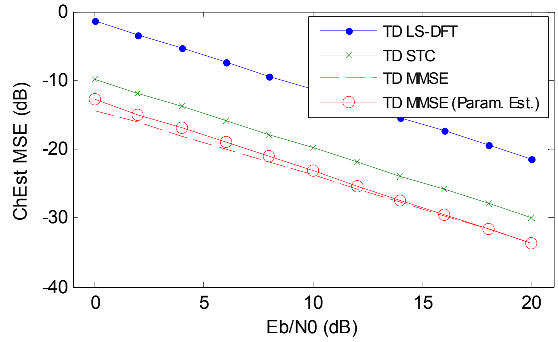

Figure 6. Channel estimation MSE (outdoor scenario).

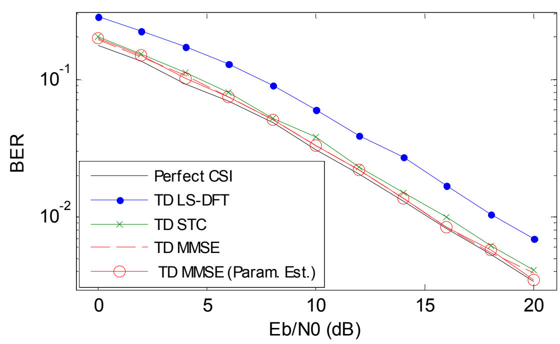

Figure 7. System BER performance (outdoor scenario).

noted as "Perfect CSI" represents the situation where the perfect channel state information (CSI) is used in the decision block.

On both scenarios, the method in [13] and the proposed method present a consistent performance. The method in [13] always achieves the worst performance due to the fact that it does not take advantage of the channel characteristics; in the indoor scenario, $\approx 16dB$ and $\approx 14,5dB$ degradation in the channel estimation MSE when compared with the proposed method for the lower and higher values of Eb/N0, respectively ($\approx 3dB$ and $\approx 2,5dB$ in the BER results); in the outdoor scenario, $\approx 13dB$ and $\approx 12dB$ degradation in the channel estimation MSE when compared with the proposed method for the lower and higher values of Eb/N0, respectively ($\approx 3dB$ and $\approx 2,5dB$ in the BER results).

In opposition, the proposed method always achieves the best performance with a BER performance near the ideal perfect CSI. It presents the ability of dealing with the increasing channel delay spread by always weighing the energy of channel taps vs. noise variance.

The performance of the method in [12] is closely dependent on the channel delay spread. Its performance is bond by the 2 previous methods. A channel with a short delay spread will result in the best performance (by having the CIR energy concentrated in just a few taps, most of the noise is eliminated in the estimation process). As the channel delay spread increases, the performance tends to that of the method in [13].

Results show that the MMSE filter using the estimated parameters presents a performance near the ideal situation were the filter used the true channel correlation and noise variance.

V. CONCLUSIONS

We have presented a pilot sequence design and associated TD MMSE channel estimation algorithm for OFDM systems. The investigated method eliminates the use of DFT/IDFT operation before the estimation process, resulting in an undemanding structure with very low computational load.

It was demonstrated that the operations up to the CIR estimate can be equivalently performed in TD with a simple linear operation. By working in TD, the estimation of MMSE filter parameters is simplified when compared with the FD counterpart. A simple method to estimate the required filter's parameters is introduced and its performance evaluated by simulations. Results show that the performance degradation is negligible when compared with the ideal MMSE filter.

ACKNOWLEDGMENT

The authors wish to thank Fundação para a Ciência e a Tecnologia that partially supported this work through the project "PHOTON - Distributed and Extendible Heterogeneous Radio Architectures using Fibre Optic Networks" (PTDC/EEA-TEL/72890/2006).

REFERENCES

[1] R. V. Nee, R. Prasad, *OFDM for Wireless Multimedia Communications*, 1st edition, Artech House, 2000.

[2] G. L. Stuber, J. R. Barry, S. W. McLaughlin, Y. Li, M. A. Ingram and T. G. Pratt, "Broadband MIMO-OFDM

wireless communications," *Proceedings of the IEEE*, vol. 92, no. 2, pp. 271–294, Feb. 2004.

[3] A. J. Paulraj, D. A. Gore, R. U. Nabar and H. Bolcskei, "An overview of MIMO communications - a key to gigabit wireless," *Proceedings of the IEEE*, vol. 92, no. 2, pp. 198–218, Feb. 2004.

[4] J.-J. van de Beek, O. Edfors, M. Sandell, S. K. Wilson, P. O. Borjesson, "On channel estimation in OFDM systems," in *Proc. IEEE Vehicular Technology Conference*, pp. 815 – 819, Chicago, USA, July 1995.

[5] P. Hoeher, S. Kaiser, P. Robertson, "Two-dimensional pilot-symbol-aided channel estimation by Wiener filtering," in *Proc. ICASSP97*, Munich, Germany, pp. 1845-1848, April 1997.

[6] Y. Li, L. J. Cimini, N. R. Sollenberger, "Robust channel estimation for OFDM systems with rapid dispersive fading," *IEEE Transactions on Communications*, vol. 46, pp. 902 – 915, July 1998.

[7] B. Yang, K. B. Letaief, R. S. Cheng, Z. Cao, "Channel estimation for OFDM transmission in multipath fading channels based on parametric channel modeling," *IEEE Transactions on Communications*, vol. 49, pp. 467 – 478, March 2001.

[8] Y. Li, Z. Li, Y. Cai, Y. Xu, "An improved channel estimation scheme for OFDM systems by tracking the subspace," in *Proc. IEEE PIMRC'03*, vol. 2, pp. 1109 – 1113, Beijing, China, Sept. 2003.

[9] O. Simeone, Y. Bar-Ness, U. Spagnolini, "Pilot-based channel estimation for OFDM systems by tracking the delay-subspace," *IEEE Trans. on Wireless Communications*, vol. 3, pp. 315 – 325, Jan. 2004.

[10] C. S. Yeh, Y. Lin, "Channel estimation using pilots tones in OFDM systems," *IEEE Transactions on Broadcasting*, vol. 45, pp. 400-409, December 1999.

[11] H. Minn, V. Bhargava, "An investigation into time-domain approach for OFDM channel estimation," *IEEE Transactions on Broadcasting*, vol. 46, no. 4, pp. 240-148, December 2000.

[12] C. Ribeiro, A. Gameiro, "Direct time-domain channel impulse response estimation for OFDM-based systems," in *Proc. IEEE Vehicular Technology Conference*, Baltimore, USA, Oct. 2007.

[13] A. Chini, M. S. El-Tanany, S. A. Mahmoud, "Transmission of high rate ATM packets over indoor radio channels," *IEEE Journal on Selected Areas in Communications*, vol. 14, nº4, April 1996.

[14] A. Chini, "Multicarrier modulation in frequency selective fading channels," Ph.D. dissertation, Carleton University, Canada, 1994.

[15] O. Edfors, "Low-complexity algorithms in digital receivers," Ph.D. dissertation, Lulea University of Technology, Sweden, 1996.

[16] S. Kay, *Fundamentals of Statistical Signal Processing*, Englewood Cliffs, NJ, USA, Prentice-Hall, 1998.

[17] T. Yucek, H. Arslan, "Delay spread and time dispersion estimation for adaptive OFDM systems," in *Proc. Wireless Communications and Networking Conference*, vol.3, pp.1433-1438, Las Vegas, USA, 2006.

Carlos Ribeiro received his Licenciatura (five year course) and his MSc in Electronic Engineering from the University of Coimbra in 1996 and 2003 respectively. He is currently an Assistant Lecturer in the Polytechnic Institute of Leiria, and a researcher at the Instituto de Telecomunicações - Pólo de Aveiro. His research interests lie in signal processing for multicarrier communication systems. He is currently working in his PhD in schemes for joint channel estimation and synchronization for multicarrier systems.

Atílio Gameiro received his Licenciatura (five years course) and his PhD from the University of Aveiro in 1985 and 1993 respectively. He is currently a Professor in the Department of Electronics and Telecommunications of the University of Aveiro, and a researcher at the Instituto de Telecomunicações - Pólo de Aveiro, where he is head of group. His main interests lie in signal processing techniques for digital communications and communication protocols. Within this research line he has done work for optical and mobile communications, either at the theoretical and experimental level, and has published over 100 technical papers in International Journals and conferences. His current research activities involve space-time-frequency algorithms for the broadband component of 4G systems and joint design of layers 1 and 2.